Biophysical Characterization of a β-Peptide Bundle:

Comparison to Natural Proteins

*E. James Petersson[†], Cody J. Craig[†], Douglas S. Daniels[†], Jade X. Qiu[†] & Alanna Schepartz[†‡]**

Departments of [†]Chemistry and [‡]Molecular, Cellular and Developmental Biology,

Yale University, New Haven, Connecticut 06520-8107 USA

General Methods. The synthesis and HPLC purification of Zwit-1F have been described previously.[1] Zwit-1F concentrations were determined by the absorbance of the Zwit-1F solution at 257.5 nm ($\varepsilon_{257.5}$ = 390 $M^{-1}cm^{-1}$)[2] using a Beckman B640 UV/visible spectrophotometer (Beckman, Fullerton, CA). The low absorbance of Zwit-1F in at 257.5 nm prohibited dilution into denaturing conditions for most concentration determinations; however, trial two-fold dilutions of 400 μM Zwit-1F into buffer or 8M guanidinium hydrochloride to yield 200 μM solutions gave UV absorbances that differed by only 5%. Circular dichroism (CD) spectra were acquired with a Jasco J-810 Spectropolarimeter (Jasco, Tokyo, Japan) equipped with a Peltier temperature control. Analytical ultracentrifugation (AU) was performed using a Beckman XL-I instrument. Differential scanning calorimetry experiments were performed on a Microcal VP-DSC instrument (Northhampton, MA) in the labs of Dr. Jeff Hoch at the University of Connecticut Health Center (Farmington, CT). ^{1}H NMR experiments were performed on a Bruker 500 MHz instrument. All experiments were performed in phosphate buffer (10 mM NaH_2PO_4, 200 mM NaCl, pH adjusted to 7.1 with NaOH) except as noted.

Calculation of Table 1 Parameters. Surface areas were computed from the crystal structures listed in Table S1 according to Lee and Richards[3] using the buried_surface script in CNS.[4] Buried interaction surfaces were computed with the following formula: Nmer surface area – (N • Monomer surface area). $\Delta G_{area} = (-RT\ln K_a)/(\text{Buried Surface Area})$

Table S1. Surface Area Calculations

		Surface Area (Å^2)				
Protein (PDB ID)	n	Monomer	Oligomer	Buried	$\ln K_a$	ΔG_{area}
Zwit-1F[1]	8	1, 591	5, 592	7, 136	71.0	5.9[a]
Hemerythrin[5] (2HMQ)	8	5, 891	32, 128	15, 000	84.0[6]	3.3[a]
Aldolase[7] (1ADO)	4	15, 970	54, 007	9, 883	64.5[8]	3.9[a]
GCN4[9] (2ZTA)	2	3, 265	4, 765	1, 765	14.3[10]	4.8[a]
ROP[11] (1ROP)	2	4, 359	6, 002	2, 716	≥ 13.8[12]	≥ 3.0[a]

[a] ΔG_{area} in units of cal•mol^{-1}•Å^{-2}.

Circular Dichroism. Wavelength-dependent CD spectra were obtained in phosphate buffer at 25 ºC in continuous scan mode with a 1 nm data pitch, 50 nm/min scanning speed, 4 sec response, 1 nm band width, and 3 accumulations. The CD spectra of Zwit-1F at concentrations between 12.5 μM and 400 μM used to produce the points in Figure 1B are shown in Figure S1A. The concentration dependence of the molar residue elipticity (MRE) at 205 nm was determined by least-squares fitting of the total Zwit-1F monomer concentration as a function of experimental MRE with the following equation in Kaleidagraph (Synergy Software; Reading, PA):

$$[\text{Zwit-1F}]_{Total} = \left\{ \frac{(MRE_{Exp} - MRE_{Mon})(1/K_a)}{n(MRE_{Nmer} - MRE_{Mon})\left[1 - \left(\frac{(MRE_{Exp} - MRE_{Mon})}{(MRE_{Nmer} - MRE_{Mon})}\right)\right]^n} \right\}^{1/(n-1)}$$

See DeGrado and Lear[13] for a derivation of this equation. The values obtained for the fitted parameters were MRE_{Mon} = 314 ± 300 deg•cm^2•dmol^{-1}, MRE_{Nmer} = 9862 ± 335 deg•cm^2•dmol^{-1}, and $\ln K_a$. = 70.5 ± 1.9. The black curve in Figure 1C was produced using these parameters.

The temperature-dependent CD spectra were obtained at 205 nm, between 5 and 95 °C, using the variable temperature module provided with the instrument. Data were collected with a 1 °C data pitch, 5 s. delay time, 1 °C/min. temperature slope, 4 s. response time, and 1 nm band width. The first derivatives of the temperature-dependent CD spectra for Zwit-1F at 50, 100, 200, and 300 μM are shown in Figure S1B. The T_m values reported in the main text correspond to the temperature at which $dMRE_{205}/dT$ is a maximum.

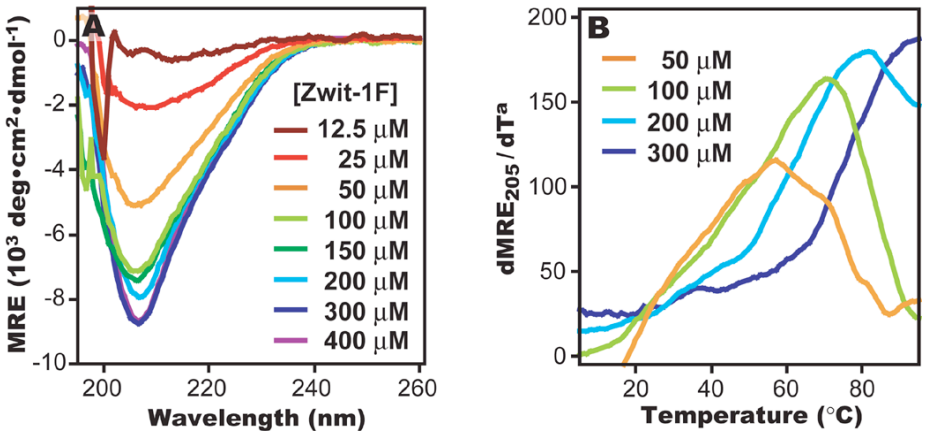

Figure S1. (A) Zwit-1F wavelength-dependent CD spectra at varying concentrations in phosphate buffer at 25 °C. MRE = molar residue elipticity. (B) Plot of the first derivative of MRE_{205} with respect to temperature for the Zwit-1F concentrations indicated. [a] $dMRE_{205}/dT$ in units of deg•cm^2•dmol^{-1}•K^{-1}.

Sedimentation Equilibrium. Samples analyzed using analytical ultracentrifugation were prepared by dissolving HPLC-purified and lyophilized β-peptides in phosphate buffer at the desired concentrations (75 μM, 150 μM, and 300 μM). The samples were then centrifuged to equilibrium at 25 °C at three different speeds (42,000, 50,000, and 60,000 rpm) in an AN 60-Ti 4-hole rotor equipped with six-channel, carbon-epoxy composite centerpieces supplied by Beckman. Absorbance was monitored at 230 nm. Data were collected with a 0.001 cm step size, and successive scans were initiated at 2-hour intervals. Samples were judged to have reached equilibrium when no significant change in radial concentration was observed in 3

successive scans using the program Match within the Heteroanalysis software suite (available from the National Analytical Ultracentrifugation Facility website, http://vm.uconn.edu/~wwwbiotc/uaf.html). The partial specific volume of Zwit-1F was calculated from the functional group composition according to Durchschlag and Zipper.[14] The data were fit to a monomer-Nmer equilibrium model using Heteroanalysis software. The results of a representative global fitting are: Fixed parameters: monomer MW = 1636 Da, $\overline{V}$ = 0.812 cm^3/g, d = 1.0074 g/mL , ε_{230} = 980 $M^{-1} \bullet cm^{-1}$, and n = 8; Fitted parameters: $\ln K_a$ = 71.0 ± 0.9, baseline deviation < 0.02. Figure S2 shows data fit with these parameters and the resulting residuals.

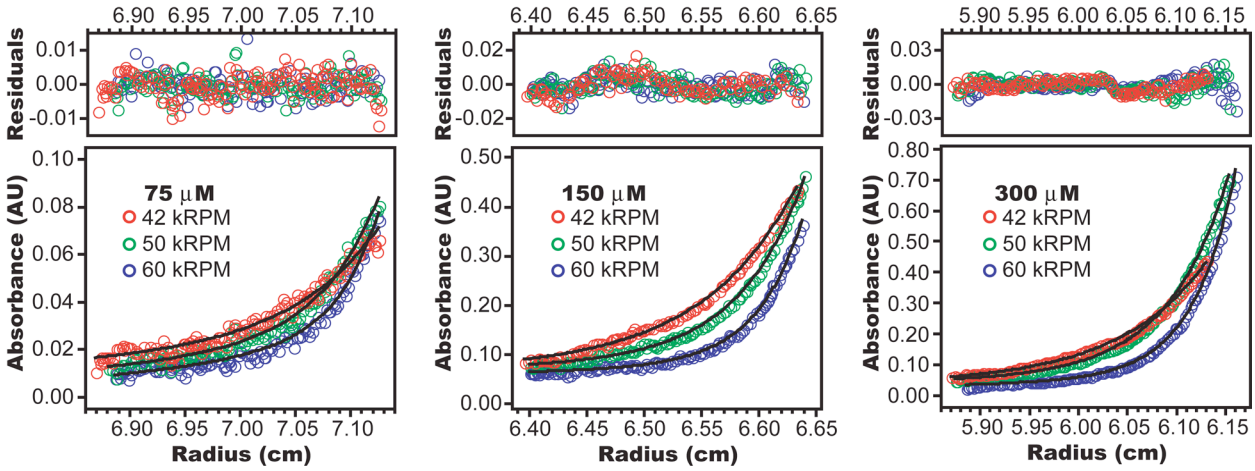

Figure S2. Zwit-1F Sedimentation Equilibrium Analysis. Samples containing 75 µM, 150 µM, or 300 µM Zwit-1F monomer were prepared in phosphate buffer and centrifuged to equilibrium at speeds of 42, 000 (red), 50, 000 (green), or 60, 000 RPM (blue) at 25 °C. Experimental data are shown as points; lines indicate a fit to a monomer-octamer model as described.

Differential Scanning Calorimetry. Temperature scans were performed from 5 to 125 °C at a scan rate of 1 °C/min. with a 10 min. equilibration period at 5 and 125 °C. All scans were performed with an excess pressure of 40 PSI. Samples of 300 μL (142 μL sample cell) were injected from the autosampling tray after being held at 10 °C. The raw data of temperature, power, and time were converted to plots of heat capacity versus temperature. This data was fit to a two-state model with dissociation of eight subunits using the program EXAM.[15] This process

involves fitting $\Delta H(T_{1/2})$, $\Delta C_P(T_{1/2})$, $\Delta C_P'(T_{1/2})$, $T_{1/2}$, B_A, B_A', B_B, B_B' in the following equations where N and n are fixed (a thorough derivation is given in NIST Technical Note 1401[15]):

For the transition $A \rightleftharpoons nB$, the heat required to melt N moles is

$$\frac{dQ}{dT} = (1-\alpha)\left[B_A + B'_A(T - T_{1/2})\right] + N\left(\frac{\Delta H(T)^2}{RT^2}\right) f(\alpha) + \alpha\left[B_B + B'_B(T - T_{1/2})\right]$$

where N_A is the number of moles of A, N_B is the number of moles of B and $f(\alpha) = \frac{\alpha(1-\alpha)}{n(1-\alpha)+\alpha}$

and $\alpha = 1 - \frac{N_{A,T}}{N_{A,T=0}} = \frac{N_{B,T}}{N_{B,T=\infty}}$. The free energy is determined relative to $T_{1/2}$ using

$$\frac{K}{K_{T_{1/2}}} = \frac{\frac{(\alpha N_{B,T=\infty})^n}{(1-\alpha)N_{A,T=0}}}{\frac{(1/2\, N_{B,T=T_{1/2}})^n}{(1-1/2)N_{A,T=T_{1/2}}}} = \frac{(2\alpha)^n}{2(1-\alpha)} = e^{-\frac{\Delta\Delta G}{RT}}$$ where $\alpha = 1/2$ at $T_{1/2}$.

$\Delta\Delta G$ is determined by the following thermodynamic equations:

$$\Delta H(T) = \Delta H(T_{1/2}) + \Delta C_P(T_{1/2})(T - T_{1/2}) + 1/2\Delta C_P'(T - T_{1/2})^2 \qquad \Delta C_P(T) = \Delta C_P(T_{1/2}) + \Delta C_P'(T - T_{1/2})$$

$$-\frac{\Delta\Delta G}{T} = \left(\frac{\Delta H(T_{1/2})}{T_{1/2}}\right)\left(\frac{T - T_{1/2}}{T}\right) + \Delta C_P(T_{1/2})\left(\ln\frac{T}{T_{1/2}} - \frac{T - T_{1/2}}{T}\right) + 1/2\Delta C_P'\left(\frac{(T + T_{1/2})(T-T_{1/2})}{T} - 2T_{1/2}\ln\frac{T}{T_{1/2}}\right)$$

The fitting results are shown in Figure 2B (for 300 μM Zwit-1F) and Figure S3 (for 250 and 350 μM Zwit-1F). The value of the equilibrium constant at 25 °C ($K = 5.3 \times 10^{-31}$) was calculated using $K(T) = 1/(K(T_{1/2})\bullet e^{-\Delta\Delta G/RT})$, where $K(T_{1/2}) = (C_T/2)^n/(C_T/2n)$ and C_T is the total peptide concentration. DSC curves were also obtained at 150 and 200 μM Zwit-1F. The fitted parameters from these data sets are summarized in Table S2. The temperature dependence of ΔH was globally fit to $\Delta H(T) = \Delta H(T_{1/2}) + \Delta C_P(T_{1/2})\bullet(T-T_{1/2}) + 1/2\Delta C_P'\bullet(T-T_{1/2})^2$ with $\Delta C_P'$ set to -0.0129 kcal•mol^{-1}•K^{-2}, the average value from individual DSC trials, yielding: ΔH(89.1 °C) = 107.6 kcal•mol^{-1} and ΔC_P(89.1 °C) = 0.7 kcal•mol^{-1}•K^{-1} ($\Delta H + \Delta C_P(T)$ Fit). $\Delta H(T)$ was also fit to $\Delta H(T) = \Delta H(T_{1/2}) + \Delta C_P(T_{1/2})\bullet(T-T_{1/2})$, yielding: ΔH(89.1 °C) = 107.5 kcal•mol^{-1} and ΔC_P(89.1 °C) = 0.9 kcal•mol^{-1}•K^{-1} ($\Delta H + \Delta C_P$ Fit).

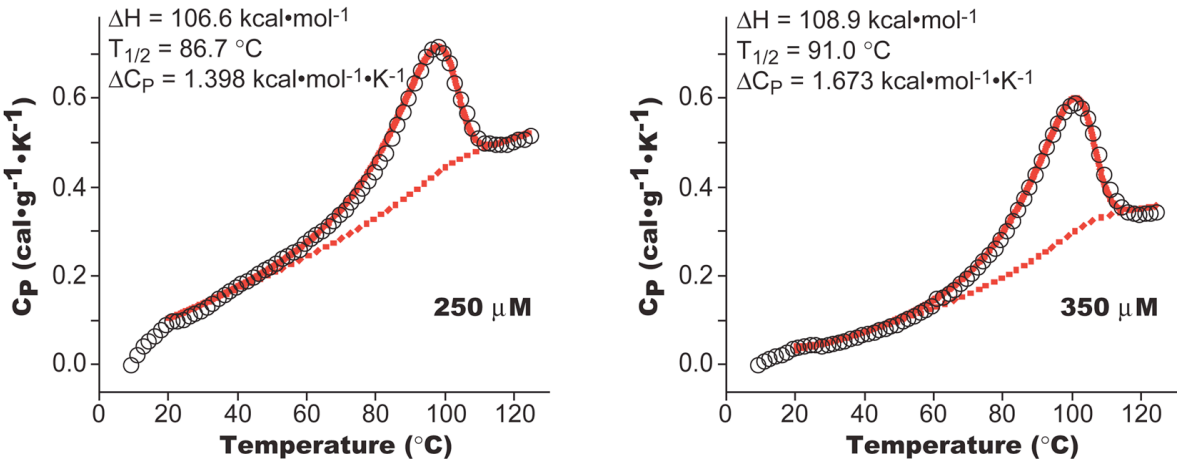

Figure S3. DSC analysis of 250 and 350 μM Zwit-1F unfolding fit to two state model with subunit dissociation. Raw data is shown as black circles. The baseline change in heat capacity is shown as a dotted red line and the fitted heat capacity function is shown as a solid red line.

We note a discrepancy between the globally fitted ΔC_P(89.1 °C) value and the ΔC_P obtained from the individual fit at 300 μM (where $T_{1/2}$ = 89.1°C, see Table S2). There is substantial precedent for inaccuracies in ΔC_P terms obtained from individual fits.[16, 17] Additionally, we expect that further DSC study will better establish baseline heat capacity changes for β-peptides allowing us to improve our fit as Privalov[18] updated Freire's GCN4 work (see below).[17]

Table S2. DSC Parameters from Fit with EXAM[15]

[Zwit-1F]	$T_{1/2}$(°C)	$\Delta H(T_{1/2})$	$\Delta C_P(T_{1/2})$	ΔC_P'
150 μM	79.3	101.1	0.9	- 14
200 μM	83.8	101.6	1.3	- 103
250 μM	86.7	106.6	1.4	- 97
300 μM	89.1	107.3	1.4	- 270
350 μM	91.0	108.9	1.7	- 163
$\Delta H + \Delta C_P$ Fit		107.5	0.9	—
$\Delta H + \Delta C_P(T)$ Fit		107.6	0.7	- 129*

ΔH in units of kcal•mol^{-1}. ΔC_P in units of kcal•mol^{-1}K^{-1}. ΔC_P' in units of 10^{-4} kcal•mol^{-1}•K^{-2}. * Fixed.

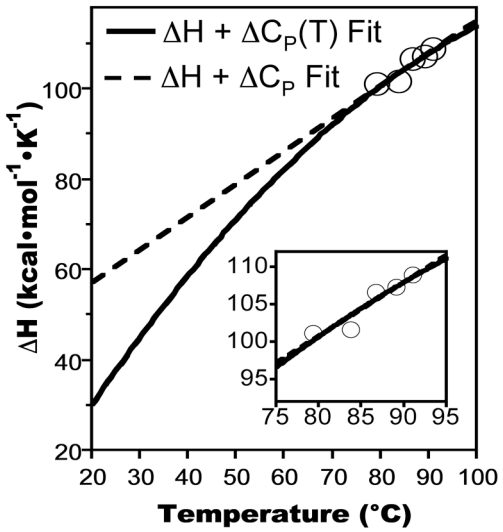

Figure S4. Global fitting of the temperature dependence of ΔH (data taken from Table S2) to the equation $\Delta H(T) = \Delta H(T_{1/2}) + \Delta C_P(T_{1/2})\bullet(T-T_{1/2}) + 1/2\Delta C_P'\bullet(T-T_{1/2})^2$, where $T_{1/2}$ = 89.1 °C and ΔC_P' = 0 or -129 x 10^{-4} kcal•mol^{-1}•K^{-2}.

The integrated calorimetric enthalpy (ΔH_{Cal}) was calculated by integrating the area between the baseline and the fitted heat capacity between 20 and 120 °C. This value was compared to the equivalent ΔH_{Cal} for GCN4 reported by Freire and coworkers, 31.5 kcal•mol^{-1}•K^{-1} monomer or 7.7 cal•g^{-1}•K^{-1} (MW = 4096 Da).[17] Dragan and Privalov later report a larger value for ΔH_{Cal}, obtained by assigning a baseline heat capacity for the folded state based on measurement of the heat capacity of bovine pancreatic trypsin inhibitor (BPTI).[18] BPTI is a highly disulfide cross-linked helical protein used as a model for the effects of heating a helix which cannot unfold. This baseline falls substantially below the heat capacity curve of the folded state of GCN4, which Freire and coworkers used as a baseline. Consequently, Dragan and Privalov obtain a much higher ΔH_{Cal} value, 79 kcal•mol^{-1}•K^{-1} monomer or 19.3 cal•g^{-1}•K^{-1}. As we have no such model for the heating of a folded β-peptide helix, our baseline is more analogous to that employed by Freire and coworkers, and thus we compare to their ΔH_{Cal} value.

Deuterium Exchange NMR Studies. All spectra were acquired at 25 °C using the WATERGATE solvent suppression pulse sequence ZZPWG. Before acquisition under the WATERGATE pulse sequence, a standard proton spectrum was taken and the position of the water peak was determined. The transmitter offset (^{01}P) was set to this frequency for ZZPWG acquisitions. Post processing was performed with a *sfil* type baseline correction set to 1.5 ppm and a line broadening factor of 5.0. The sample was dissolved in phosphate buffer prepared using a 9:1 mixture of H_2O and D_2O. The ^{1}H NMR spectrum of a 1.5 mM Zwit-1F sample was invariant over a period of three months, showing that our spectra correspond to a stable species in solution. For deuterium exchange studies, a 1.5 mM solution of peptide was lyophilized and re-dissolved in phosphate-buffered D_2O just prior to insertion in the instrument. Any peptide that could not be resolubilized was removed from the solution by centrifugation at 13,000 RPM

for 1 minute before addition to the NMR tube. Phosphate-buffered D_2O was prepared by lyophilizing phosphate buffer made with H_2O and re-dissolving the salt in D_2O. pD was checked as below. The spectrometer was pre-locked and shimmed on an identical volume of 1.5 mM Zwit-1F in 9:1 H_2O/D_2O before the deuterium exchange experiment was initiated. The deuterium exchange spectra were acquired and processed in the same fashion as described for the fully protonated spectra except that the *sfil* post-processing algorithm was not necessary.

Exchange rates were determined by comparing the height of the amide peaks at 8.65 ppm (A), 8.35 ppm (B), 8.07 ppm (C), or 7.97 ppm (D) to the area of a non-exchanging aromatic peak at 6.70 ppm. Peak positions were determined relative to (2,2,3,3-d_4) trimethyl-3-propionic acid (at 1 mM), referenced to 0 ppm. Data from three trials were averaged and fit to $H(t) = H_0e^{-k_{ex}t}$ using Kaleidagraph (Synergy Software; Reading, PA); where H(t) is the normalized peak height and H_0 and k_{ex} are fitted parameters. The exchange rates (k_{ex}) thus determined are: A: 1.6 X 10^{-4} s^{-1}, B: 1.2 X 10^{-4} s^{-1}, C: 2.9 X 10^{-4} s^{-1}, and D: 0.6 X 10^{-4} s^{-1}. Results obtained by lyophilizing Zwit-1F from phosphate solution (made with H_2O) and re-dissolving it in D_2O were not substantially different, although more insoluble peptide was observed.

As amide exchange rates vary logarithmically with pD in the EX2 regime (pH < 9.5 for most α-amino acid proteins), the sample pD must be carefully monitored.[19] We verified that our experiments fall into the EX2 regime by measuring exchange at pD 5 to demonstrate the pD dependence of k_{ex} (k_{ex}(pD 5) = 10^{-5} – 10^{-6}). To ensure that reconstitution of lyophilized samples in D_2O did not affect the buffering ability of the phosphate solution, we measured the pD of NMR samples after exchange was complete using an Orion 98-26 pH meter (Thermo Fisher Scientific Inc., Waltham, MA) in the labs of Prof. Pat Loria (Yale University) to be 6.84 ± 0.8 pH units, which corresponds to a corrected pD of 7.24.[20]

Deuterium exchange is often characterized by a protection factor (P) equal to k_{rc}/k_{ex}, where k_{rc} is the exchange rate of an amide N-H in a random coil under similar conditions. According to Bai *et al.*, the intrinsic exchange rate for amide protons in a random coil (using a poly-D,L-Ala peptide standard) is $k_{rc} = 4.3\ s^{-1}$ at 25 °C and pD = 7.2 in 0.5 M KCl.[21] Assuming that this value represents a reasonable estimate of the intrinsic exchange rate for an amide proton in an unstructured β-peptide, we calculate a protection factor ($P = k_{rc}/k_{ex}$) of 7×10^4 for Zwit-1F. Alternatively, one may use the exchange rate of poly-β-homoglycine (β-alanine) as a standard. The rates of exchange have been measured by Glickson and Applequist at pH 3 - 6 at 12 °C.[22] We used the equations below to obtain the exchange rate at various pHs and temperatures.

$$k_{rc} = k_a[D^+] + k_b[OD^-] + k_w$$

For βG_n, $k_a = 11.2\ s^{-1}$

$k_b = 9.3 \times 10^6\ s^{-1}$

$k_w = 0$ and $-\log K_w = 14.7$ at 12 °C.

$$\text{where } k_n(T) = k_n(T°) \cdot e^{\frac{-E_n}{R}\left(\frac{1}{T} - \frac{1}{T°}\right)}$$

$E_a, E_b = 14, 17\ kcal \cdot mol^{-1}$

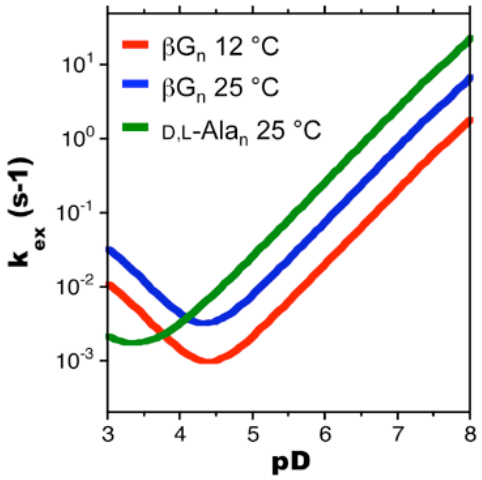

Figure S4. The pH dependence of poly-D,L-Ala at 25 °C from Bai *et al.*[21] and poly-βG at 12 °C calculated using the k_a, k_b, and k_w values given above, taken from Glickson and Applequist.[22] The pH dependence of poly-βG at 25 °C calculated using the activation energies for the acid-catalyzed exchange rate (E_a) and base-catalyzed exchange rate (E_b) from Bai *et al.*[21]

The pH-dependence of k_{rc} for poly-D,L-Ala at 25 °C and poly-βG at 12 °C or 25 °C is shown in Figure S5. We calculate $k_{rc} = 1.2\ s^{-1}$ at pH 7.2 and 25 °C for poly-βG, which corresponds to a protection factor of $2 \times 10^4\ s^{-1}$ for Zwit-1F.

In addition to the βG standards used in calculating P, initial studies with a poorly structured variant of Zwit-1F, Acid-1Y^{A2,11}, clearly show that slow exchange is not an intrinsic property of β-peptides. Figure S6B shows the amide region of Acid-1Y^{A2,11} at 100 μM concentration in dilute buffer (1 mM each NaH_2PO_4, borate, and citrate, pH 7.0) prepared with 9:1 H_2O/D_2O. Figure S6C shows the same sample 10 min. after redissolution in D_2O following lyophilization.

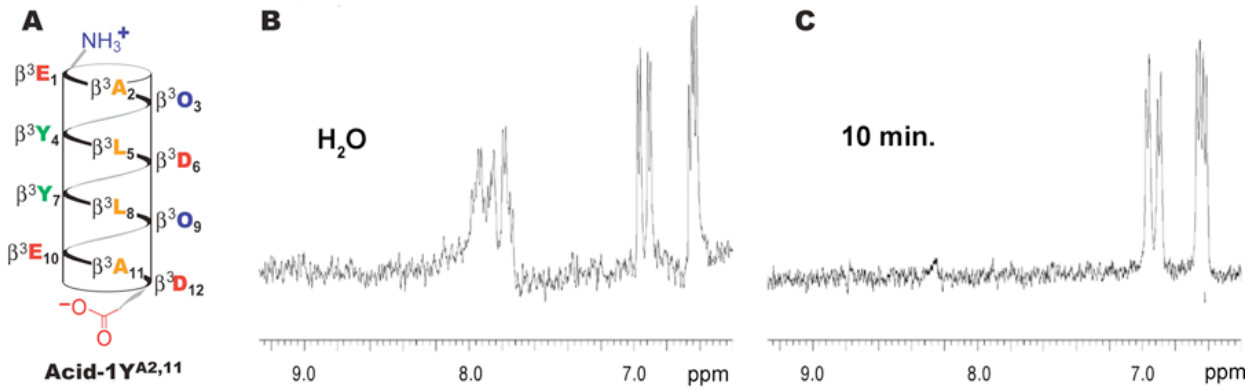

Figure S6. (A) Helical net representation of Acid-1Y^{A2,11}. β^3-amino acids are designated by α-amino acid letter code. O signifies ornithine. 500 MHz ^{1}H NMR spectra of 100 μM Acid-1Y^{A2,11}, acquired in (B) dilute phosphate buffer prepared with "H_2O" (9:1 H_2O/D_2O) or (C) 10 minutes after reconstitution in D_2O of a lyophilized Acid-1Y^{A2,11} sample. The small peak at 8.2 ppm is a contaminant that does not exchange.

8-Analino-1-naphthalenesulfonate (ANS) Studies. Increased ANS fluorescence in the presence of a protein is used commonly to diagnose a loosely folded hydrophobic core.[23, 24] Stock solutions of 1.2 mM Zwit-1F were prepared in phosphate buffer; a 20 μM stock of ANS was prepared in the same buffer (from an initial stock of 20 mM ANS in 1:1 H_2O/CH_3CN). Binding reactions were performed by mixing 50 μL of the ANS solution with an appropriate volume of the Zwit-1F stock solution and diluting to a final volume of 100 μL with phosphate buffer. High Zwit-1F concentration data points were obtained by dilution of a 200 μM ANS stock. Fluorescence intensity (counts/s) measurements were made using a Photon Technology International (Lawrenceville, NJ) Quantamaster C-60 spectrofluorimeter at 25 °C in a 1 cm path length Hellma (Müllheim, Germany) cuvette. The sample was excited with 350 nm light (4 nm

slit width) and fluorescence emission was measured at 1 nm intervals between 400 and 600 nm. The ratio of ANS fluorescence in the presence and absence of peptide was found to increase linearly with Zwit-1F concentration from 1.1 at 12.5 μM to over 100 at 1 mM. The fact that this increase was linear implies that ANS interacts with monomeric Zwit-1F rather than oligomeric Zwit-1F. Moreover, this fluorescent adduct was insoluble; centrifugation at 13,000 rpm precipitated it from solution. In contrast, Zwit-1F analogs Acid-1F (β^3O_{10} to β^3E_{10}) and Base-1F (β^3E_1 to β^3O_{10}) do not significantly bind ANS at concentrations up to 400 μM, either alone or in a 1:1 mixture.

References

1. Daniels, D. S.; Petersson, E. J.; Qiu, X. J.; Schepartz, A., *J. Am. Chem. Soc.* **2007,** 129, 1532-1533.
2. Fasman, G. D., *Handbook of Biochemistry and Molecular Biology, Proteins*, 3rd ed., CRC Press, **1976**, 183-203.
3. Lee, B.; Richards, F. M., *J. Mol. Biol.* **1971,** 55, 379-387.
4. Brunger, A. T.; Adams, P. D.; Clore, G. M.; DeLano, W. L.; Gros, P.; Grosse-Kunstleve, R. W.; Jiang, J. S.; Kuszewski, J.; Nilges, M.; Pannu, N. S.; Read, R. J.; Rice, L. M.; Simonson, T.; Warren, G. L., *Acta Crystallogr. D* **1998,** 54, 905-921.
5. Holmes, M. A.; Stenkamp, R. E., *J. Mol. Biol.* **1991,** 220, 723-737.
6. Langerman, N. R.; Klotz, I. M., *Biochemistry* **1969,** 8, 4746-4757.
7. Blom, N.; Sygusch, J., *Nat. Struct. Biol.* **1997,** 4, 36-39.
8. Tolan, D. R.; Schuler, B.; Beernink, P. T.; Jaenicke, R., *Biol. Chem.* **2003,** 384, 1463-1471.
9. O'Shea, E. K.; Klemm, J. D.; Kim, P. S.; Alber, T., *Science* **1991,** 254, 539-544.
10. Wendt, H.; Baici, A.; Bosshard, H. R., *J. Am. Chem. Soc.* **1994,** 116, 6973-6974.
11. Banner, D. W.; Kokkinidis, M.; Tsernoglou, D., *J. Mol. Biol.* **1987,** 196, 657-675.
12. Munson, M.; Balasubramanian, S.; Fleming, K. G.; Nagi, A. D.; Obrien, R.; Sturtevant, J. M.; Regan, L., *Protein Sci.* **1996,** 5, 1584-1593.
13. Degrado, W. F.; Lear, J. D., *J. Am. Chem. Soc.* **1985,** 107, 7684-7689.
14. Durchschlag, H.; Zipper, P., *Prog. Colloid Polym. Sci.* **1994,** 94, 20-39.
15. Kirchhoff, W. M., *NIST Technical Note 1401*, **1993**.
16. Lassalle, M. W.; Hinz, H. J.; Wenzel, H.; Vlassi, M.; Kokkinidis, M.; Cesareni, G., *J. Mol. Biol.* **1998,** 279, 987-1000.
17. Thompson, K. S.; Vinson, C. R.; Freire, E., *Biochemistry* **1993,** 32, 5491-5496.
18. Dragan, A. I.; Privalov, P. L., *J. Mol. Biol.* **2002,** 321, 891-908.
19. Krishna, M. M. G.; Hoang, L.; Lin, Y.; Englander, S. W., *Methods* **2004,** 34, 51-64.
20. Glasoe, P. K.; Long, F. A., *J. Phys. Chem.* **1960,** 64, 188-190.
21. Bai, Y. W.; Milne, J. S.; Mayne, L.; Englander, S. W., *Proteins: Struct., Funct., Genet.* **1993,** 17, 75-86.
22. Glickson, J. D.; Applequist, J., *J. Am. Chem. Soc.* **1971,** 93, 3276-3281.
23. Lumb, K. J.; Kim, P. S., *Biochemistry* **1995,** 34, 8642-8648.
24. Goto, Y.; Fink, A. L., *Biochemistry* **1989,** 28, 945-952.